

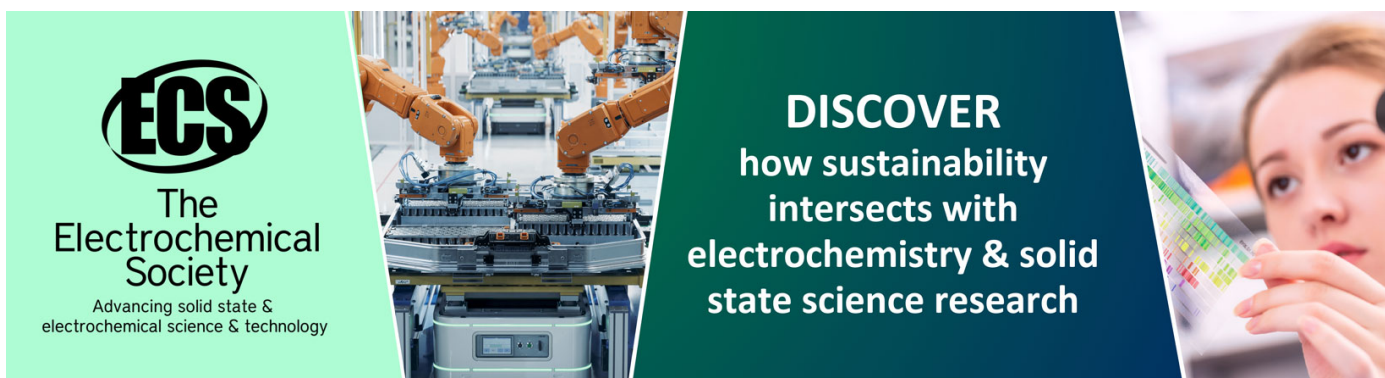
Energy relaxation of localized excitons at finite temperature

To cite this article: S A Tarasenko *et al* 2001 *Semicond. Sci. Technol.* **16** 486

View the [article online](#) for updates and enhancements.

You may also like

- [The applicability of the transport-energy concept to various disordered materials](#)
S D Baranovskii, T Faber, F Hensel et al.
- [Comparison of two methods simulating inter-track interactions using the radiobiological Monte Carlo toolkit TOPAS-nBio](#)
Larissa Derksen, Sebastian Adeberg, Klemens Zink et al.
- [A dual center study to compare breath volatile organic compounds from smokers and non-smokers with and without COPD](#)
A Gaida, O Holz, C Nell et al.



ECS
The
Electrochemical
Society
Advancing solid state &
electrochemical science & technology

DISCOVER
how sustainability
intersects with
electrochemistry & solid
state science research

Energy relaxation of localized excitons at finite temperature

S A Tarasenko¹, A A Kiselev^{1,2}, E L Ivchenko¹, A Dinger³,
M Baldauf³, C Klingshirn³, H Kalt³, S D Baranovskii⁴,
R Eichmann⁵ and P Thomas⁵

¹ Ioffe Physico-Technical Institute, 26 Polytekhnicheskaya Str., St Petersburg 194021, Russia

² North Carolina State University, Raleigh, NC 27695-7911, USA

³ Institut für Angewandte Physik, Universität Karlsruhe, D-76128 Karlsruhe, Germany

⁴ Institut für Physikalische Chemie, Philipps-Universität Marburg, D-35032 Marburg, Germany

⁵ Fachbereich Physik, Philipps-Universität Marburg, D-35032 Marburg, Germany

Received 9 January 2001, accepted for publication 9 April 2001

Abstract

Macro- and micro-photoluminescence (PL) spectroscopy has been applied to investigate the exciton localization in cubic CdS/ZnSe type-II superlattices (SL) in the temperature range 5–35 K. The non-monotonic shift of the macro-PL peak with increasing temperature reveals the kinetic contribution of acoustic-phonon-assisted exciton multi-hopping processes. The experimental data are described by means of computer simulation and calculations based on a kinetic theory generalized from zero to finite temperatures. The advantages of each theoretical approach are discussed.

1. Introduction

The spectral peak of photoluminescence (PL) from undoped quantum well (QW) structures at low temperatures is usually red-shifted with respect to the peak in absorption or PL-excitation (PLE) spectra. This so-called Stokes shift is explained taking into account that the excitation spectrum is dominated by optical transitions to extended free-exciton states, while the low-temperature PL arises from radiative recombination of excitons localized by interface microroughness and substitutional alloy disorder (see [1–6] and references therein). In the multiple-hopping regime, the population of the exciton-band tail and, hence, the PL spectrum are formed as a result of competition between the exciton recombination and acoustic-phonon-assisted hopping from one localization site to another.

The kinetic theory of localized excitons in the zero-temperature limit is based on the approximation of hopping to the nearest lower-energy neighbour site [5]. This theory has been applied to describe experimental data for ZnCdSe/ZnSe QW structures, including the cw Stokes shift between the PL and PL-excitation peaks, the time decay of the PL integral intensity, the temporal shift of the PL spectral maximum in time-resolved experiments and the shapes of cw and transient PL spectra [7]. Baranovskii *et al* [8] used the Monte-Carlo simulation procedure to model the same scenario and obtained (for the identical set of parameters) an excellent agreement

between the simulation and the kinetic analytical theory [7]. They employed a similar simulation technique for finite temperatures and confirmed the non-monotonic temperature dependence of the cw PL peak, demonstrated previously by Zimmermann *et al* [9]. Physically, this curious phenomenon can be explained (see also [10]) taking into account that at $T = 0$ the PL is dominated by excitons finding themselves at accidentally isolated localization sites acting as pores. For such sites (or traps) the lifetime with respect to hopping to the nearest lower-energy neighbour exceeds the recombination time. At low, but finite temperatures, an exciton trapped by an effective pore has an opportunity for further energy relaxation by hopping first to the nearest higher-energy neighbour and then to a deeper-energy site. The non-monotonic behaviour of the Stokes shift (retained even with the temperature-induced shift of the band gap subtracted) has also been observed experimentally [10–12]. A generalized kinetic equation for excitons localized in QW structures at finite temperatures has been proposed by Golub *et al* [5], but up to now this equation has not been applied to analyse the temperature evolution of the PL spectra.

In this paper, we report on an experimental study of macro- and micro-PL (μ -PL) spectra of CdS/ZnSe multi-layer structures, a novel II–VI heteropair [13, 14], with focus on the temperature dependence of the PL peak. The low temperatures used made it possible to ignore the thermal activation of excitons from localized to extended states. The obtained experimental data are described in terms of the multi-hopping

model by using two independent theoretical approaches, namely, exact computer simulation and approximate kinetic theory. Comparison between theory and experiment furnishes the best-fit parameters of localized excitons in the CdS/ZnSe heterostructures, and that between the results of the two calculations gives notion of the validity of the kinetic theory.

The paper is organized as follows. The next section displays the experimental results. Computer simulation and comparison with the experiment are the topics of section 3. The kinetic theory is presented in section 4. Section 5 is devoted to simulation of μ -PL spectra.

2. Experimental macro- and μ -PL spectra

The properties of localized excitons in several cubic CdS/ZnSe superlattices (SLs) were investigated by means of spatially integrated (macro-PL) and spatially resolved (μ -PL) photoluminescence spectroscopy. The band alignment of this heterostructure is of type II, with the conduction and valence band off-sets of around 800 meV and 500 meV, respectively [13]. The CdS (ZnSe) layers form potential wells for electrons (holes). The high structural quality of the superlattices has been confirmed by the observation of higher-order folded acoustic and confined optical phonons in Raman scattering experiments [14–16]. In this work, we concentrate on macro- and μ -PL from a 200-period (19 Å/19 Å) CdS/ZnSe superlattice grown by molecular beam epitaxy on GaAs(001), with CdS and ZnSe as source materials [17].

For the PL measurements, a sample was mounted in a liquid helium flow cryostat equipped with a resistive heater, allowing the sample temperature to be maintained between 5 K and 300 K with an accuracy of ± 0.1 K. An excitation source served the 351 nm line of an Ar⁺-ion laser, with excitation intensity of about 2 W cm^{-2} . The spectra discussed in what follows were taken with spatial resolution of $\sim 1 \mu\text{m}$ (μ -PL) or $\sim 50 \mu\text{m}$ (macro-PL). The signal was dispersed by a 75-cm double spectrometer and detected with a Peltier-cooled CCD, with spectral resolution of $\sim 50 \mu\text{eV}$. Macro-PLE spectra were taken using a tunable 1 m monochromator to select the excitation lines from the spectrum of a 200 W xenon lamp. Owing to intensity problems, the spectral resolution had to be restricted to $\sim 4 \text{ meV}$ in this special case.

Figure 1 shows a macro-PL spectrum (full curve) of the SL, recorded at 5 K. The spectrum has a full width at half-maximum (FWHM) of around 22 meV. Additionally, a PLE spectrum is displayed in the inset, together with a macro-PL spectrum. The detection energy for the PLE spectrum shown here was chosen to be at the PL-peak. The resonance in the PLE spectrum is attributed to the heavy-hole 1s-exciton transition, which is in good agreement with the calculated transition energy. No other resonances were observed, most probably because of the strong damping of these states. The Stokes shift was estimated from the energy difference between the PL- and PLE-maxima to be 18 meV.

As already mentioned in previous publications, we observe a strong non-monotonic (red–blue–red) shift of the macro-PL peak with increasing temperature [15, 18]. This behaviour is typical of all the investigated CdS/ZnSe superlattices. In the following, we concentrate on the temperature range between 5 K and 35 K, where the first red

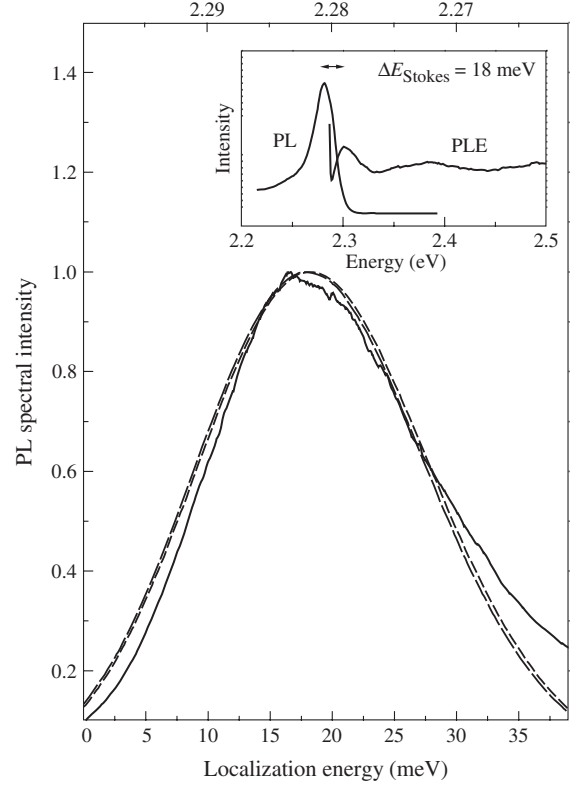


Figure 1. PL spectrum taken from a CdS/ZnSe 19 Å/19 Å SL and recorded with spatial resolution of $\sim 50 \mu\text{m}$ at 5 K (full curve). The other two curves represent the results of computer simulation at $T = 0$ (broken) and $T = 5$ K (dotted) for the parameter set given in the text, with the simulated spectrum inhomogeneously broadened. In the inset, the PL and PLE spectra are compared, revealing a Stokes shift of 18 meV.

shift is observed for the sample under study and the kinetics of localized excitons is of importance.

In figure 2, three selected μ -PL spectra recorded at different temperatures are shown. The spectra are normalized with respect to the PL-peak and shifted vertically against each other for clarity. In addition to a broad PL background, a structure of narrow superimposed lines is observed (FWHM $\approx 300 \mu\text{eV}$), typical of strongly localized excitons forming quasi-zero-dimensional states. Within the experimental accuracy, the shift of the peak with increasing temperature is identical for all the lines and corresponds to the temperature-induced shift of the superlattice band gap. The shift between 5 K and 35 K amounts to -1.4 meV . Above 35 K, the narrow line emission is hardly observable, indicating enhanced delocalization of excitons. Macro-PL spectra show a more pronounced red shift of the emission peak (-3.5 meV) with the temperature increasing from 5 to 35 K. This effect, also seen for the envelope of the μ -PL spectra, is clear evidence in favour of phonon-assisted exciton hopping to deeper localized states.

The full circles in figure 3 show the measured temperature dependence of the relative shift of the PL peak

$$\Delta E_m = \hbar\omega_m(T) - \hbar\omega_m(0) - \delta E_g(T), \quad (1)$$

normalized to the PL Stokes shift at $T = 0$. Here, $\omega_m(T)$ is the spectral position of the PL peak at temperature T , and

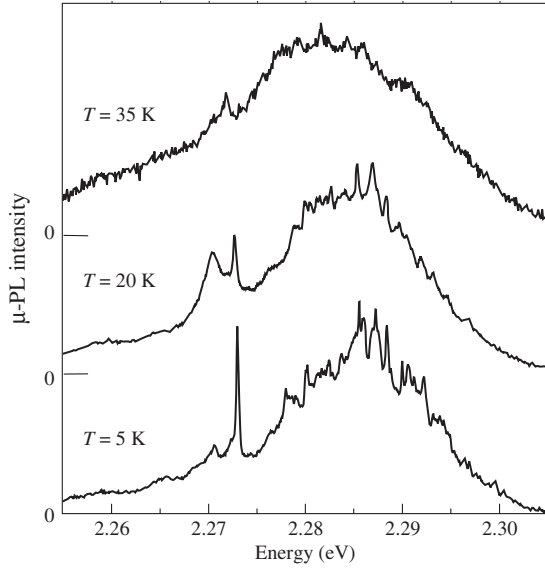


Figure 2. Temperature dependent μ -PL spectra (spatial resolution $\approx 1 \mu\text{m}$) taken from a $19 \text{ \AA}/19 \text{ \AA}$ CdS/ZnSe SL.

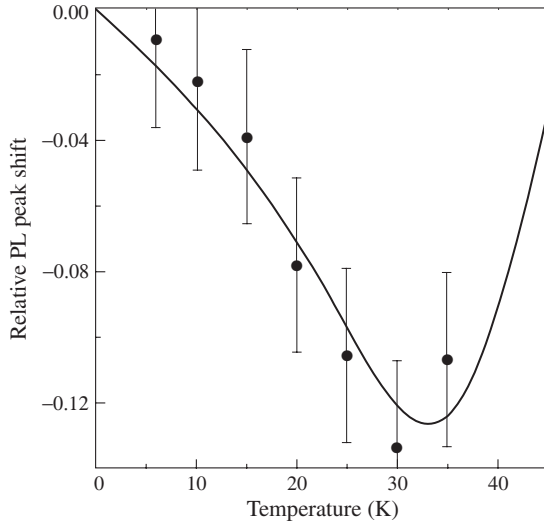


Figure 3. Temperature dependence of the PL-peak shift in accordance with equation (1), normalized to the low-temperature PL Stokes shift of 18 meV for a $19 \text{ \AA}/19 \text{ \AA}$ CdS/ZnSe SL. Full circles, experiment; full curve, computer simulation for the same parameters as in figure 1.

$\delta E_g(T)$ is the temperature shift of the narrow lines in the μ -PL spectra. The definition of ΔE_m excludes the effect of temperature dependence of the band gaps, and ΔE_m represents a purely kinetic contribution to the shift.

A large value of the macro-PL Stokes shift and the observation of a superimposed system of narrow lines in the μ -PL spectra unambiguously demonstrate the localized nature of recombining excitons. The thickness of 19 \AA for both CdS and ZnSe layers is small enough for excitons in these type-II heterostructures to have large binding energy and, therefore, a remarkable oscillator strength. On the other hand, 19 \AA is wide enough to ignore the heavy-hole tunneling through the CdS barrier. Thus, the $19 \text{ \AA}/19 \text{ \AA}$ CdS/ZnSe heterostructure can be considered a superlattice only for a conduction-band

electron, and a multiple quantum well for a heavy photohole confined within a particular ZnSe layer. It follows then that, in order to describe the above experimental data, one needs to consider two-dimensional (2D) hopping of localized excitons and sum up independently the PL intensities related to different ZnSe layers.

3. Computer simulation: comparison with experiment

We start with a list of notation used in what follows. The exciton localization energy denoted by ε is positive and is related to the exciton excitation energy, E , and the exciton mobility edge, E_0 , by

$$\varepsilon = E_0 - E; \quad (2)$$

$w(\varepsilon, \varepsilon', r)$ is the exciton transfer rate of the $\varepsilon \rightarrow \varepsilon'$ transition between sites separated by distance r . As in [8], we assume that

$$w(\varepsilon, \varepsilon', r) = \omega_0 \exp\left(-\frac{2r}{a} - \frac{\varepsilon - \varepsilon' + |\varepsilon - \varepsilon'|}{2k_B T}\right) \quad (3)$$

where a is the localization length, T is temperature, k_B is Boltzmann's constant and ω_0 is a constant factor. The exciton recombination time is labelled as τ_0 , with its dependence on ε ignored. $g(\varepsilon)$ is the exciton density of states, and the concentration of sites with localization energy exceeding ε is given by

$$\rho(\varepsilon) = \int_{\varepsilon}^{\infty} g(\varepsilon') d\varepsilon'.$$

$\Gamma_0(\varepsilon)$ is the generation rate into the state ε from delocalized states. In the following, we neglect the dependence of Γ_0 on ε and assume an exponential density of states

$$g(\varepsilon) = g_0 \exp\left(-\frac{\varepsilon}{\varepsilon_0}\right) \quad (4)$$

and thus $\rho(\varepsilon) = \varepsilon_0 g(\varepsilon) = g_0 \varepsilon_0 \exp(-\varepsilon/\varepsilon_0)$.

For numerical simulation, we generate 2D random uniform distributions of localization sites, $(\mathbf{r}_i, \varepsilon_i)$, $i = 1 \dots n$, on a square cell of size $L = (n/g_0 \varepsilon_0)^{1/2}$. Here $\mathbf{r}_i = (x_i, y_i)$ are the space positions of the sites and ε_i are the localization energies generated with the chosen function of energy density of states, $g(\varepsilon)$. The number of sites, n , or the ratio $L/a = (n/g_0 \varepsilon_0 a^2)^{1/2}$ is taken large enough to obtain results insensitive to further increase in the L value. The exponential decay of the transition rates with intersite distance permits moderate values of L/a and relatively small numbers of localization states, n , in the configuration, $n = 1000$ and $L/a = 44.3$ for the particular parameter set as listed below. To minimize the effects of the cell perimeter even further, we use periodic boundary conditions for the configuration of sites by identifying the opposite sides of the cell. This is taken into account by assuming the effective distance between sites \mathbf{r}_i and \mathbf{r}_j to have the form $r_{ij} = \sqrt{x_{ij}^2 + y_{ij}^2}$, where

$$x_{ij} = \begin{cases} |x_i - x_j| & \text{if } |x_i - x_j| \leq L/2 \\ |x_i - x_j| - L/2 & \text{if } |x_i - x_j| > L/2 \end{cases}$$

and y_{ij} is defined likewise. For a given site configuration, all the possible intersite transition rates (3) are calculated and substituted into the set of n linear rate equations for the occupation numbers f_i , $i = 1 \dots n$,

$$\left[\sum_{j \neq i} w(\varepsilon_i, \varepsilon_j, r_{ij}) + \frac{1}{\tau_0} \right] f_i - \sum_{j \neq i} w(\varepsilon_j, \varepsilon_i, r_{ji}) f_j = \Gamma_0 \quad (5)$$

which can be written as a single $n \times n$ -matrix equation. The stationary generation from delocalized to localized states is assumed to be the same for all the localization sites and small enough to enable the dependence of transition rates on the occupation of final states to be ignored. The matrix kinetic equation (5) is solved and the occupation numbers f_i are found for a series of M site configurations. The PL spectrum is then calculated as the sum

$$J(\omega) = \sum_{m=1}^M \sum_{i=1}^n f_i^{(m)} \delta(\omega - \omega_i^{(m)}) \quad (6)$$

where the index m enumerates the configurations from 1 to M , $\omega_i^{(n)}$ is the resonance frequency of the i th localized-exciton state in the m th configuration, and the function $\delta(\Omega)$ describes the homogeneous broadening of a single line. It is taken in the Lorentzian form

$$\delta(\Omega) = \frac{1}{\pi} \frac{\gamma}{\gamma^2 + \Omega^2}.$$

While simulating macroscopic PL spectra, we generate ≥ 200 configurations to obtain a sufficiently smooth spectrum. The number of configurations taken for simulation of μ -PL spectra is much smaller, so that we have a system of narrow lines superimposed on the smooth spectral background.

In order to qualitatively take into account the inhomogeneous broadening, the macroscopic PL spectra $J_0(E_0 - \hbar\omega)$ simulated for a fixed value of the exciton mobility edge E_0 are convoluted with a Gaussian

$$J(\hbar\omega) \propto \int dE_0 F(E_0 - \bar{E}_0) J_0(E_0 - \hbar\omega) \\ F(E_0 - \bar{E}_0) = \frac{1}{\sqrt{\pi}\Delta} \exp\left[-\left(\frac{E_0 - \bar{E}_0}{\Delta}\right)^2\right]. \quad (7)$$

The dimensionless parameters chosen to calculate the PL spectra are the following: $\omega_0\tau_0 = 10^3$ and $\pi(a/2)^2 g_0 \varepsilon_0 = 0.4$. The inhomogeneous broadening is described by the Gaussian (7) with $\Delta = 2 \varepsilon_0$. At zero temperature, the PL peak occurs at $\varepsilon_m \equiv E_0 - \hbar\omega_m = 3.38\varepsilon_0$ for the homogeneous mobility edge E_0 and at $3.53 \varepsilon_0$ if the inhomogeneous broadening is included. Since the PL Stokes shift equals 18 meV (see the inset of figure 1), we obtain for ε_0 a value of $(18/3.53) \approx 5.1$ meV.

In addition to the above simulation procedure, we also applied the Monte-Carlo simulation method described in detail by Baranovskii *et al* [8] to check the accuracy of the calculations. The simulation parameter combinations $\omega_0\tau_0$ and $\pi(a/2)^2 g_0 \varepsilon_0$ were the same as in the calculation described above. Sample sizes were 10 000 sites and 250 000 sites for a finite size check. To average over different realizations of the disorder, we used up to 200 000 samples and checked

for the convergence of our results. We found both methods to give identical results. Note that the computing time is temperature independent in the first computer simulation. As for the Monte-Carlo method, it is faster for lower and slower for higher temperatures.

Figures 1 and 3 compare qualitatively the results of computer simulation with the experimental data. Low-temperature macro-PL spectra are shown in figure 1, with the full curve representing the spectrum measured for the 19 Å/19 Å CdS/ZnSe SL at $T = 5$ K, and the broken and dotted curves corresponding to the computer-simulated PL spectra for $T = 0$ and $T = 5$ K, respectively. Figure 3 shows the purely kinetic contribution to the temperature-induced shift of the PL spectral maximum, with the full curve being the result of computer simulation and full circles representing the behaviour of the experimental PL-peak in accordance with equation (1). It can be seen that the results of computer simulation performed with the parameter set listed above are in good agreement with the experimental data.

4. Kinetic theory: comparison with computer simulation

The kinetic theory of localized excitons at zero temperature [5, 7] was derived in the approximation of optimal hopping transfers. This means that an exciton is allowed to hop to a lower-energy site characterized by the maximum value of $w(\varepsilon, \varepsilon', r)$, which, at zero temperature, depends in the model under consideration only on r , see equation (3). At finite temperatures, in the framework of the approximation of optimal hopping transfers, each site is characterized by three parameters $\varepsilon, \varepsilon'$ and r [5]. Here ε is the localization energy for a given site, while ε' and r are the localization energy and the distance to an optimum site characterized by a maximum value of $w(\varepsilon, \varepsilon', r)$ in the given local configuration. If the occupation probability of such a state is denoted by $f(\varepsilon, \varepsilon', r)$, then the energy distribution $N(\varepsilon)$ determining the PL spectral intensity

$$J(\hbar\omega) \propto N(E_0 - \hbar\omega) \quad (8)$$

is related to $f(\varepsilon, \varepsilon', r)$ by

$$N(\varepsilon) = g(\varepsilon) \int_0^\infty d\varepsilon' \int_0^\infty dr P_\varepsilon(\varepsilon', r) f(\varepsilon, \varepsilon', r). \quad (9)$$

Here $P_\varepsilon(\varepsilon', r)$ is the distribution of optimal neighbours in energy and space. For uncorrelated localized sites distributed in a 2D space we can write

$$P_\varepsilon(\varepsilon', r) = 2\pi r g(\varepsilon') \exp[-U(\varepsilon, \varepsilon', r)] \quad (10)$$

$$U(\varepsilon, \varepsilon', r) = \int_\Omega \int d\varepsilon_2 dr_2 2\pi r_2 g(\varepsilon_2) \quad (11)$$

with the integration performed over the area Ω in the (ε_2, r_2) space, where

$$w(\varepsilon, \varepsilon_2, r_2) > w(\varepsilon, \varepsilon', r).$$

If the correlation between the successive hopping events is ignored, the kinetic equation for $f(\varepsilon, \varepsilon', r)$ has the form

$$\left[\frac{1}{\tau_0} + w(\varepsilon, \varepsilon', r) \right] f(\varepsilon, \varepsilon', r) - \int_0^\infty \int_0^\infty d\varepsilon_1 dr_1 \frac{g(\varepsilon_1)}{g(\varepsilon)} \\ \times P_{\varepsilon_1}(\varepsilon, r_1) w(\varepsilon_1, \varepsilon, r_1) f(\varepsilon_1, \varepsilon, r_1) = \Gamma_0. \quad (12)$$

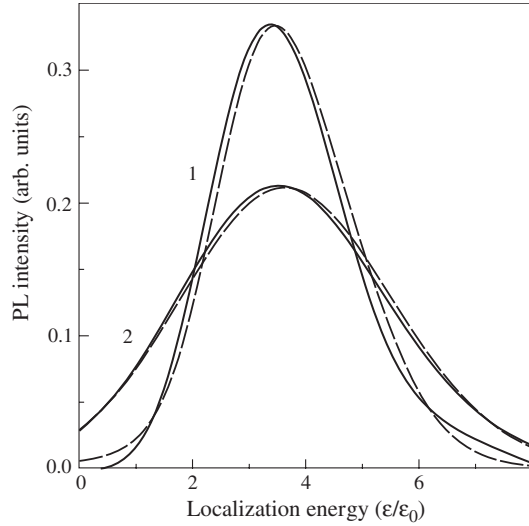


Figure 4. Theoretical low-temperature PL spectra obtained by computer simulation (full curves) and calculated in terms of the proposed kinetic theory in the absence (1) and presence (2) of inhomogeneous broadening.

The terms in the left-hand side describe, respectively, the exciton recombination, transfer to the optimal site ε' and generation from the state $(\varepsilon_1, \varepsilon, r_1)$. At zero temperature

$$w(\varepsilon, \varepsilon', r) = w_0 \exp\left(-\frac{2r}{a}\right) \theta(\varepsilon' - \varepsilon)$$

$$P_\varepsilon(\varepsilon', r) = 2\pi r g(\varepsilon') \exp[-\pi r^2 \rho(\varepsilon)] \theta(\varepsilon' - \varepsilon)$$

where $\theta(x)$ is the Heaviside step function. It then follows that at $T = 0$ we can use the pair (ε, r) , instead of three parameters, to characterize the localized state, and equation (12) reduces to

$$\left[\frac{1}{\tau_0} + w(r)\right] f(\varepsilon, r) - \int_0^\varepsilon g(\varepsilon_1) d\varepsilon_1 \int_0^\infty 2\pi \times r_1 dr_1 \exp[-\pi r_1^2 \rho(\varepsilon_1)] w(r_1) f(\varepsilon_1, r_1) = \Gamma_0. \quad (13)$$

In figure 4, we compare zero-temperature PL spectra furnished by computer simulation and calculated in terms of the kinetic theory by equation (13). Spectra 1 correspond to a fixed exciton mobility edge, and spectra 2 are obtained by convolution of the PL spectra 1 with the Gaussian (7).

Figure 5(a) presents the relative shift of the PL peak as a function of temperature, calculated with the inhomogeneous broadening neglected. The broken curve is obtained by using the numerical solution of equation (12). It can be seen that a rather simple kinetic theory leads to a non-monotonic temperature dependence of the PL-peak shift. Moreover, the agreement between the broken and full (simulation) curves is both qualitative and quantitative. Some discrepancy in the PL spectra and, hence, in the PL-peak behaviour can be attributed to the following two approximations of the kinetic theory: it ignores transfers to non-optimal sites and the correlation between the successive hops. At zero temperature the correlation is insignificant [5], which clearly follows from the excellent agreement between the two curves in figure 4. At finite temperatures the role of correlations increases. In fact, at nonzero, but low temperature, part of excitons participating in upward hopping transitions from site O to O' return

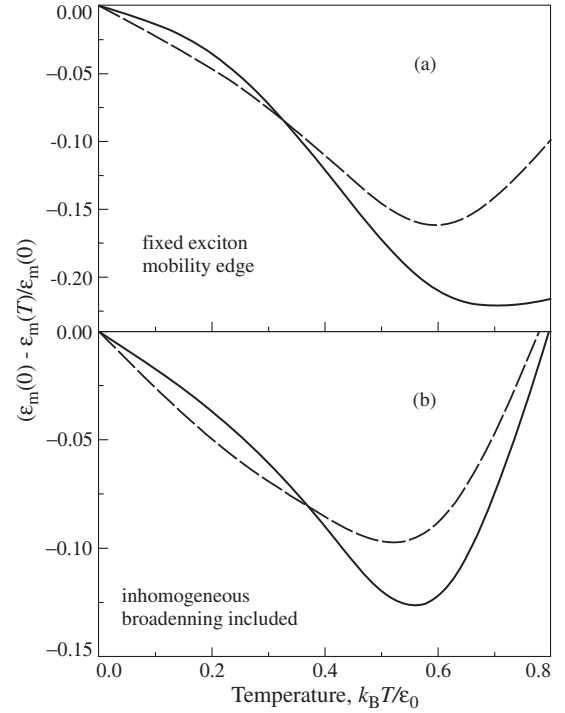


Figure 5. Relative shift of the PL peak as a function of temperature, calculated (a) neglecting and (b) taking into account the inhomogeneous broadening. Full curves, computer simulation; broken curves, kinetic theory.

back to site O and either recombine at this site or relax to other localization sites O_1 different from O and O' . A better agreement in the framework of the kinetic theory could be achieved by going beyond the approximation of optimal hoppings (see [19] for details) and/or taking into account the hopping correlation. However, in this case the kinetic equation would have a much more complicated form and its application would lose some obvious advantages over the computer simulation procedure.

To illustrate and to make the physics of the PL-peak temperature behaviour more transparent, let us consider three sites O , O' and O_1 with localization energies ε , ε' and ε_1 ($\varepsilon' < \varepsilon < \varepsilon_1$), assuming the initial exciton generation to occur only to site O . Then the steady-state occupancies f , f' and f_1 of these three sites satisfy the following set of rate equations

$$\begin{aligned} (\tau_0^{-1} + w_{O'O} + w_{O_1O}) f - w_{OO'} f' &= G_O \\ (\tau_0^{-1} + w_{O_1O'} + w_{OO'}) f' - w_{O'O} f &= 0 \\ \tau_0^{-1} f_1 - w_{O_1O} f - w_{O_1O'} f' &= 0 \end{aligned} \quad (14)$$

Here G_O is the rate of generation to site O , $w_{\alpha\beta}$ is the hopping rate for the acoustic-phonon assisted transition from site β to site α , and the upward transitions $O_1 \rightarrow O$ and $O_1 \rightarrow O'$ are ignored. If site O is a pore at zero temperature, then $w_{O_1O} < \tau_0^{-1}$. Let site O' be the optimal at $T \neq 0$ with respect to O , which means that $w_{O'O} > w_{O_1O}$. Site O_1 is assumed to satisfy the condition $w_{O_1O'} > w_{OO'}$. It can be shown that, under the above assumptions and for $w_{O'O} > \tau_0^{-1}$, the ratio $f_1/(f + f')$ is given approximately by the product $\tau_0 w_{O'O}$. At $T = 0$, i.e. for vanishing $w_{O'O}$, this ratio is equal to $\tau_0 w_{O_1O}$, which is small compared with $\tau_0 w_{O'O}$. Thus, the

average exciton energy does shift downwards (the localization energy shifts upwards) with allowance made for the effective relaxation channel $O \rightarrow O' \rightarrow O_1$.

Figure 5(b) presents the temperature-induced shift of the PL peak for the PL spectrum convoluted according to equation (7). As compared with figure 5(a), the shape of the curves is changed remarkably. This effect of inhomogeneous broadening can be interpreted in the following way. If the PL spectrum calculated for the homogeneous mobility edge is *symmetric* about the peak, then the inhomogeneous broadening has no effect on the spectral peak position $\hbar\omega_m$. However, if the homogeneous PL spectrum is *asymmetric* about $\hbar\omega_m$, the inhomogeneous broadening results in a shift of the peak position. To estimate the shift of the PL peak through inhomogeneous broadening, we introduce the functions $J_0(\omega - \omega_m)$ representing the homogeneous PL spectrum peaked at ω_m and $F(\omega_m - \bar{\omega}_m)$, describing the inhomogeneous broadening of the peak position around the frequency $\bar{\omega}_m$. Then the observed PL spectrum is given by the convolution

$$J(\omega) = \int d\omega_m F(\omega_m - \bar{\omega}_m) J_0(\omega - \omega_m). \quad (15)$$

Taking J_0 in the asymmetric form

$$J_0(\omega - \omega_m) = C \exp[-A(\omega - \omega_m)^2] [1 + D(\omega - \omega_m)^3] \quad (16)$$

where the coefficient D is a measure of asymmetry and F has the form

$$F(\omega_m - \bar{\omega}_m) = \sqrt{\frac{B}{\pi}} \exp[-B(\omega_m - \bar{\omega}_m)^2] \quad (17)$$

we can show that

$$J(\omega) = C \sqrt{\frac{B}{A+B}} \exp\left(-\frac{AB(\omega - \bar{\omega}_m)^2}{A+B}\right) \times \left\{ 1 + \frac{BD}{(A+B)^2} (\omega - \bar{\omega}_m)^2 \left[\frac{3}{2} + \frac{B^2}{A+B} (\omega - \bar{\omega}_m)^2 \right] \right\}. \quad (18)$$

Assuming the asymmetry to be relatively weak, $|D|A^{-3/2} \ll 1$, we obtain that the spectral maximum of $J(\omega)$ occurs at the frequency $\omega_{\max} = \bar{\omega}_m + \delta\omega$, with the additional shift given by

$$\delta\omega = \frac{3D}{4A(A+B)}. \quad (19)$$

At zero temperature, both the calculated PL spectra in figure 4 almost coincide in shape. At a finite temperature, the asymmetries of the simulated PL spectrum and that calculated by using the kinetic theory are different. According to equation (19), this leads to different additional shifts $\delta\omega$ contributing to the full and broken curves in figure 5(b).

5. Simulation of μ -PL spectra

For the simulation of μ -PL spectra we took 50 subsystems each containing 1000 localized-exciton sites randomly distributed with equal probabilities in the 2D space (within a square area) and with weight $g(\epsilon)$ in energy. The exciton-mobility edge in each subsystem was chosen randomly in accordance with the

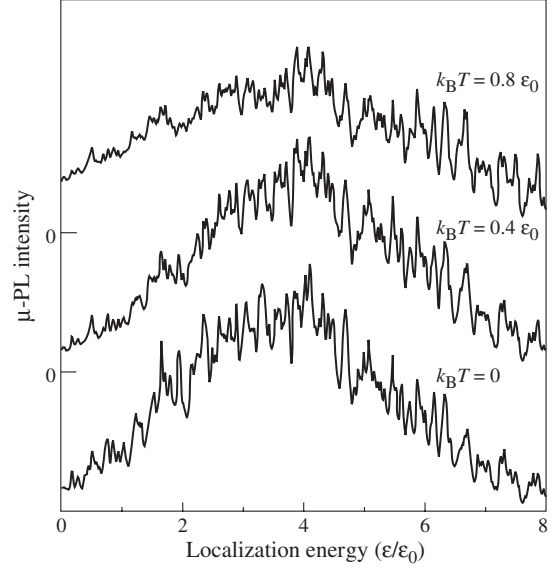


Figure 6. μ -PL spectra computer-simulated for three different temperatures. See text for details.

Gaussian distribution. Figure 6 shows the results of a computer simulation of μ -PL spectra. The spectra were calculated for the same configuration of localization sites but for different temperatures, $k_B T = 0, 0.4\epsilon_0$ and $0.8\epsilon_0$. The parameters used are the same as those in section 3, and the FWHM of a single narrow line is $2\hbar\gamma = 0.04\epsilon_0$. A smooth spectral background can be seen, reflecting the macro-PL spectrum, with a set of narrow lines corresponding to individual contributions of localization sites superimposed on it. Varying the temperature leads to exciton redistribution over the localization sites and, therefore, to changes in the intensities of the narrow lines and to evolution of the PL background. Since the bandgaps are kept constant, the energy positions of the individual narrow lines remain unchanged.

6. Summary

In conclusion, we have carried out a macro- and micro-spectroscopic study of the PL arising from radiative recombination of localized excitons in quantum well structures. The measurements have been performed on type-II multiple quantum wells for a recently grown heteropair, CdS/ZnSe. A kinetic theory developed for finite temperatures, $T < \epsilon_0$, explains the experimentally observed non-monotonic PL-peak shift with increasing temperature. The results obtained in terms of the kinetic theory are in good agreement with those furnished by computer simulation.

Acknowledgments

The work was supported by Deutsche Forschungsgemeinschaft (grants Ka761/10-1 and SFB383), Russian Ministry of Science and Russian Foundation for Basic Research (grant 98-02-18267). The high quality CdS/ZnSe SLs were grown by S Petillon and M Grün. We also wish to thank L E Golub for helpful discussions.

References

- [1] Masumoto Y, Shionoya S and Okamoto H 1985 *Proc. 17th Int. Conf. Phys. Semicond.* eds J D Chadi and W A Harrison (New York: Springer) p 349
- [2] Takagahara T 1989 *J. Lumin.* **44** 347
- [3] Kalt H, Collet J, Baranovskii S D, Saleh R, Thomas P, Dang Le Si and Cibert J 1992 *Phys. Rev. B* **45** 4253
- [4] Yang F, Wilkinson M, Austin E A and O'Donnell K P 1993 *Phys. Rev. Lett.* **70** 323
- [5] Golub L E, Ivchenko E L and Kiselev A A 1996 *J. Opt. Soc. Am. B* **13** 1199
- [6] Narukawa Y, Kawakami Y, Fujita Shizuo and Fujita Shigeo 1997 *Phys. Rev. B* **55** 1938
- [7] Golub L E, Ivanov S V, Ivchenko E L, Shubina T V, Toropov A A, Bergman J P, Pozina G R, Monemar B and Willander M 1998 *Phys. Status Solidi b* **205** 203
- [8] Baranovskii S D, Eichmann R and Thomas P 1998 *Phys. Rev. B* **58** 13081
- [9] Zimmermann R, Runge E and Grosse F 1996 *Proc. 23rd Int. Conf. Phys. Semicond. (Berlin, Germany, 1996)* ed M Scheffler and R Zimmermann (Singapore: World Scientific) p 1935
Zimmermann R and Runge R 1997 *Phys. Status Solidi a* **164** 511
Grassi Alessi M, Fragano F, Patanè A, Capizzi M, Runge E and Zimmermann R 2000 *Phys. Rev. B* **61** 10985
- [10] Skolnick M S, Tapster P R, Bass S J, Pitt A D, Apsley N and Aldred S P 1986 *Semicond. Sci. Technol.* **1** 29
- [11] Davey S T, Scott E G, Wakefield B and Davies G J 1988 *Semicond. Sci. Technol.* **3** 365
- [12] Daly E M, Glynn T J, Lambkin J D, Considine L and Walsh S 1995 *Phys. Rev. B* **52** 4696
- [13] Dinger A, Petillon S, Grün M, Hetterich M and Klingshirn C 1999 *Semicond. Sci. Technol.* **14** 595
- [14] Dinger A, Petillon S, Hetterich M, Grün M, Göppert M, Klingshirn C, Liang J, Weise B, Wagner V and Geurts J 1998 *Proc. 24th Int. Conf. Phys. Semicond. 1998* ed A Gershoni (World Scientific)
- [15] Dinger A, Becker R, Göppert M, Petillon S, Hetterich M, Grün M, Klingshirn C, Liang J, Weise B, Wagner V and Geurts J 1999 *Phys. Status Solidi b* **215** 413
- [16] Dinger A, Becker R, Göppert M, Petillon S, Grün M, Klingshirn C, Liang J, Wagner V and Geurts J 2000 *J. Crystal Growth* at press
- [17] Petillon S, Dinger A, Grün M, Hetterich M, Kazukauskas V, Klingshirn C, Liang J, Weise B, Wagner V and Geurts J 1999 *J. Crystal Growth* **201/202** 453
- [18] Dinger A, Baldauf M, Petillon S, Hepting A, Lürßen D, Grün M, Kalt H and Klingshirn C 2000 *J. Crystal Growth* at press
- [19] Kiselev A A 1998 *Semiconductors* **32** 504